World Electric Vehicle Journal

MDPI

Article

Height Control Strategy Design and Simulation of Electronic Control Air Suspension for Trucks

Hao Zhang [1,2], Hao Zhang [3,*], Leilei Zhao [3,*], Chuanjin Ou [1,2], Yuechao Liu [3] and Xiyu Shan [3]

[1] Research Institute of Highway, Ministry of Transport, Beijing 100088, China; zhang.hao@rioh.cn (H.Z.); 13061316768@163.com (C.O.)
[2] Key Laboratory of Operation Safety Technology on Transport Vehicles, Ministry of Transport, Beijing 100088, China
[3] School of Transportation and Vehicle Engineering, Shandong University of Technology, Zibo 255000, China; 17353477735@163.com (Y.L.); 17852739151@163.com (X.S.)
* Correspondence: zhanghao200067@163.com (H.Z.); zhaoll@sdut.edu.cn (L.Z.); Tel.: +86-198-6252-4322 (H.Z.)

Abstract: To address the large height error and attitude destabilization phenomenon in regulating the frame height of trucks with electronic control air suspension (ECAS), a height control strategy was designed. Firstly, the fundamental principles of height control were elucidated based on the single degree-of-freedom (DOF) vehicle model. The limitations of the classic non-linear mathematical model for the air spring were also highlighted. Thus, a dynamic model was constructed, consisting of an AEMSim model for the ECAS and a Simulink model for the truck. A frame height fuzzy controller was designed based on the fuzzy control theory to improve the height control accuracy and to solve the control conflict problem of the solenoid valves. Additionally, three typical control modes of the height and corresponding control strategies were proposed based on the practical requirements of usage scenarios for trucks. Finally, dynamic simulations were conducted under different modes. The results show that, compared to the existing switching control method, the proposed control approach can reduce height control errors by an order of magnitude and decrease the pitch angle by over 30%. The steady-state error remains nearly unchanged under the 30% variation of the sprung mass. The proposed control approach exhibits the superior control performance and robustness. It effectively reduces height errors and avoids the posture instability during the adjustment of the ECAS.

Keywords: truck; electronic control air suspension; height control strategy; co-simulation

Citation: Zhang, H.; Zhang, H.; Zhao, L.; Ou, C.; Liu, Y.; Shan, X. Height Control Strategy Design and Simulation of Electronic Control Air Suspension for Trucks. *World Electr. Veh. J.* **2024**, *15*, 273. https://doi.org/10.3390/wevj15060273

Academic Editor: Joeri Van Mierlo

Received: 3 May 2024
Revised: 17 June 2024
Accepted: 19 June 2024
Published: 20 June 2024

1. Introduction

To enhance the ride comfort of trucks [1,2], the popularization of the electronic control air suspension (ECAS) in truck chassis systems presents an irreversible development trend. The use of the ECAS to realize the height control of trucks provides users great convenience. However, the problems of the large height error and the attitude destabilization still need to be effectively solved during vehicle height control by the ECAS in the parking state. How to overcome the nonlinear characteristics during the inflation and deflation process of air springs, in order to achieve precise control of the height and the stable vehicle posture, has become a key issue in the field of ECAS research for trucks [3–6].

The construction of the dynamic model of the ECAS for trucks is the research basis for the control strategy. The dynamic model involves electric, pneumatic, and mechanical multi-energy field coupling. To address the outstanding problem of modeling the dynamic characteristics of the air spring model, many scholars have conducted extensive research and achieved fruitful research results. Typical studies include Yin Hang et al. [7] who proposed an air spring model with dual control equations of the pressure–temperature that can reflect the actual nonlinear dynamics of air springs. Zhu et al. [8] derived a nonlinear elastic force model for compressed air based on thermodynamic equations, which incorporated the viscoelastic force and friction of the rubber material of the airbag.

Xu [9] developed a model of the dynamic vertical stiffness of an air spring system with a rubber diaphragm–throttle orifice-added air chamber based on thermodynamics and fluid dynamics. Sayyaadi et al. [10] established a nonlinear air spring thermodynamic model based on the Berg model, which described the dynamics behavior of air springs in the longitudinal, transverse, and vertical directions. However, the simplification conditions of the dynamic model of the electronic control air suspension system for trucks established based on the mathematical model of the air spring are greater, which will affect the design results of the vehicle height control strategy. This leads to a reduction of the control effect in practical engineering applications.

The height control strategy of the ECAS is the key to achieving effective height control of trucks. To this day, many control theories have been applied to the research of the ECAS control. Chen, Hyunsup, et al. [11,12] used the sliding mode variable structure control, which can effectively overcome the nonlinearities and uncertainties in the process of filling and deflating air springs. Ma et al. proposed a nonlinear model predictive control method, which aims to achieve the whole-vehicle attitude control during the vehicle height adjustment control [13]. However, the above research objects mainly focus on passenger cars with minor load variations. Their control laws are more complex and require an accurate mathematical model of the controlled object. It is difficult to apply them directly to air suspension systems for trucks. Kou et al. [14] proposed different height modes based on the vehicle's varying loads and driving conditions, suggesting that choosing the appropriate driving height for the vehicle can effectively improve its performance. Li et al. [15], through investigation and research on vehicle driving conditions on highways, categorized the height modes of air suspension systems into three modes: inflation limit mode +20 mm, normal mode 0 mm, and deflation limit mode −20 mm. Akpakpavi et al. [16] attempted to apply switch control to the height control of air suspensions, but this method has some limitations. Setting the height deadband too small leads to frequent opening of the solenoid valve, which triggers the vehicle height oscillation and leads to attitude destabilization; conversely, the accuracy of the vehicle height control is poor. Hu et al. [17], by using the mixed logical dynamical (MLD) approach, proposed a novel control strategy to adjust the vehicle height by controlling the on–off statuses of the solenoid valves directly, but essentially, it still does not solve the limitations of the switch control method.

In summary, to address the problems mentioned above, it is necessary to conduct research on the refinement modeling and control strategy of the ECAS for trucks. Therefore, a more refined model of the ECAS based on the AMESim software (2020.1.) is established in this study. Then, using the fuzzy control theory, a control strategy of the ECAS for trucks is proposed and a design method of the height controller is built, to coordinate the contradiction between the height control accuracy and the attitude stability.

2. Fundamentals of Modeling for the Truck Height Control

The establishment studies of complex models usually start from simplified models that can better reflect their basic dynamic properties. To carry out AMESim-based modeling of the height control system for trucks, this section will elucidate the basic principles of vehicle height regulation and the shortcomings of the classical non-linear mathematical model of the air spring inflation and deflation system. Therefore, a comparative study between the AMESim model and the mathematical model is presented.

2.1. AMESim Model of the Single DOF Vehicle with the ECAS

Figures 1 and 2 show the air spring inflation and deflation circuit sketch and the physical model of the single degree-of-freedom (DOF) vehicle with the ECAS, respectively. In Figure 2, m_s is the sprung mass, C_s is the damping coefficient, F_a is the vertical force of the air spring, and z_s and q are the vehicle vertical displacement and the displacement excitation of the road, respectively. Based on the schematic diagram of the air spring inflation and deflation circuit and the physical model of the single DOF vehicle, a simulation model of

the single DOF vehicle with the ECAS is built in AMESim (Version 2020.1) software, as shown in Figure 3.

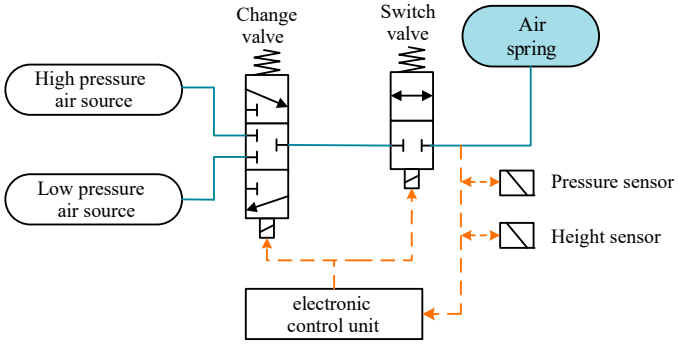

Figure 1. Air spring inflation and deflation circuit.

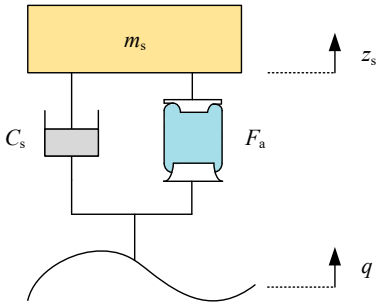

Figure 2. Physical model.

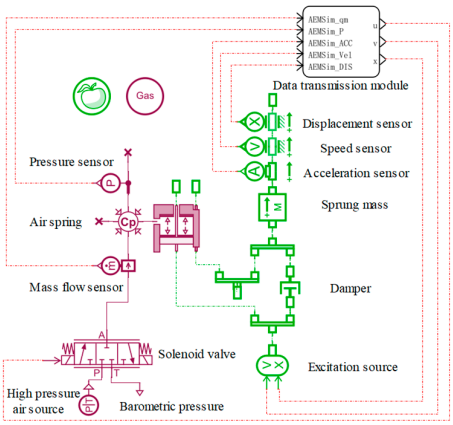

Figure 3. The simulation model of the single DOF vehicle with the ECAS.

In the model shown in Figure 3, the mechanical part is composed of the mass block, the damper, connectors, the signal input terminals, and the output terminals, which are sourced from the mechanical library provided by AMESim software. The air spring is composed of the movable cylinder piston element and the variable volume air chamber provided in the pneumatic component library. The electrical circuit part is composed of a three-position solenoid valve with three-way and a pressure-adjustable air source. The suspension status information collected by the sensors is transferred to the Simulink controller through the data transfer module. At the same time, the Simulink controller transmits the solenoid valve opening signal to the solenoid valve module. In addition, the excitation signal can be output by the Simulink module. The selection of sub-models is shown in Table 1, and the default sub-models of the software are used for the unmarked models.

Table 1. Selection of each sub-model.

Simulated Component	Sub-Model	Simulated Component	Sub-Model
High pressure air source	PNCS001	Air spring	PNRP18/PNCH012
Barometric pressure	PNAS001	Shock absorber	DAM000
Solenoid valve	PNPV003	Sprung mass	MAS002

2.2. Mathematical Model of the Single DOF Vehicle with the ECAS

Many assumptions are usually made about the air spring inflation and deflation system for mathematical modeling of the ECAS. Among them, the basic assumptions are as follows [18]:

(1) the air in the system is the ideal gas and has no gas leakage; its kinetic and potential energy are negligible; (2) the air compressor and storage tank are simplified as a high-pressure gas source, and the external environment is simplified as a low-pressure gas source, and the values of the air pressure and temperature are constant; (3) the air spring inflation and deflation process can be likened to a variable-volume adiabatic gas exchange process; (4) the gas flow through the solenoid valve is equivalent to the flow of the throttle orifices; the performance of each solenoid valve is consistent.

2.2.1. The Inflation and Deflation Model of the Air Spring

Due to the small contact surface and fast airflow with the pipe wall when the air flows through the small hole, the solenoid valve orifice can be regarded as an equivalent throttling orifice. Therefore, the nonlinear model of the airflow characteristics for the solenoid valve can be expressed as Equation (1) [19].

$$q_{\mathrm{m}} = \begin{cases} \mu p_{\mathrm{u}} A \sqrt{\dfrac{2k}{(k-1)RT_{\mathrm{u}}}\left[\left(\dfrac{p_{\mathrm{d}}}{p_{\mathrm{u}}}\right)^{\frac{2}{k}} - \left(\dfrac{p_{\mathrm{d}}}{p_{\mathrm{u}}}\right)^{\frac{k+1}{k}}\right]} & \sigma_{\mathrm{e}} < \frac{p_{\mathrm{d}}}{p_{\mathrm{u}}} < 1 \\ \mu p_{\mathrm{u}} A \sqrt{\dfrac{k}{RT_{\mathrm{u}}}\left(\dfrac{2}{k+1}\right)^{\frac{k+1}{k-1}}} & \frac{p_{\mathrm{d}}}{p_{\mathrm{u}}} \le \sigma_{\mathrm{e}} \end{cases} \tag{1}$$

where q_{m} is the mass flow rate, μ is the gas path flow resistance coefficient; A is the cross-sectional area of the throttle orifice, k is the gas adiabatic coefficient taken as 1.4, R is the gas molar constant, T_{u} is the temperature of the upstream gas; p_{u} and p_{d} are the upstream and downstream absolute pressures of the solenoid valve, respectively; and σ_{e} is the critical gas pressure ratio taken as 0.5283.

Considering that the time of the gas spring charging (discharging) process is very short when the solenoid valve is opened, the heat exchange during the gas flow process at the solenoid valve can be ignored. Therefore, the gas charging (discharging) process can be regarded as an adiabatic gas charging (discharging) process. According to the first law of thermodynamics, the absolute pressure of the gas inside the air spring can be obtained as shown in Equation (2) [20].

$$\frac{\mathrm{d}p_1}{\mathrm{d}t} = -\frac{k\beta(\dot{z}_{\mathrm{s}} - \dot{q})}{V_{10} + \beta(z_{\mathrm{s}} - q)} p_1 + \frac{kRT_2}{V_{10} + \beta(z_{\mathrm{s}} - q)} q_{\mathrm{m}} \tag{2}$$

where V_{10} is the initial volume of the air spring before inflation (deflation), β is the rate of change of the volume of the air spring, T_2 is the thermodynamic temperature of the external gas, $q_{\mathrm{m}} > 0$ represents the inflation process, and $q_{\mathrm{m}} < 0$ represents the deflation process.

2.2.2. Equations of Motion for the Single DOF Vehicle with the ECAS

According to the physical model of the single DOF vehicle with the ECAS and Equation (2), the equation of motion for the single DOF vehicle with the ECAS is established as

$$\begin{cases} m_s\ddot{z}_s = -C_s(\dot{z}_s - \dot{q}) + A_e(p_1 - p_0) - m_s g \\ \dot{p}_1 = -\dfrac{k\beta(\dot{z}_s - \dot{q})}{V_{10} + \beta(z_s - q)}p_1 + \dfrac{kRT_2q_m}{V_{10} + \beta(z_s - q)}u \end{cases} \quad (3)$$

where A_e is the effective area of the air spring, g is the acceleration of gravity, p_0 is the atmospheric pressure, and u is the opening of the proportional solenoid valve.

2.3. Comparative Analysis of the Model Differences

To verify the accuracy of the constructed AMESim air spring, an open-loop control method is adopted, where the same control signal is applied to the mathematical model and the AMESim simulation model, respectively. The values of the simulation parameters of the two models are shown in Table 2 [21], in which the control signal is a square wave signal with a period of 4.0 s, a solenoid valve opening of 20%, and a duty cycle of 35%, as shown in Figure 4. Based on the simulation data of the two models, the steady state response values of three parameters such as the displacement z_s, the absolute air pressure of the airbag, and the gas mass flow rate are extracted. The results are compared as shown in Table 3. In order to further visualize the dynamical response process and transient response differences between the two models, the time histories of these three parameters were plotted, and the results are shown in Figures 5–7.

Table 2. The model parameters of the single DOF vehicle with the ECAS.

Parameter	Value	Parameter	Value
m_s/kg	382	A_e/m^2	9.00×10^{-3}
$C_s/(N{\cdot}s{\cdot}m^{-1})$	3500	V_{10}/m^3	2.20×10^{-3}
p_1/MPa	0.41	k	1.40
p_u/MPa	0.80	$R/(J{\cdot}kg^{-1}{\cdot}K^{-1})$	287
p_0/MPa	0.10	T_u/K	298
A/m^2	3.14×10^{-6}	g	9.80

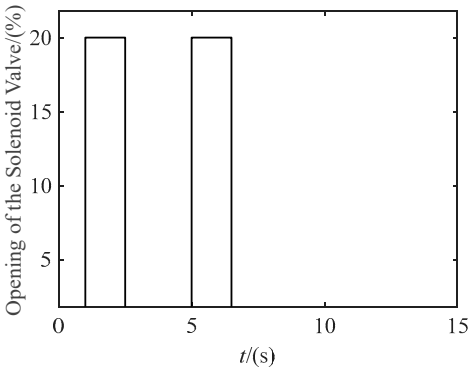

Figure 4. Control signal.

Table 3. Comparison of the simulation results.

Parameter	Mathematical Model	AMESim Model	Relative Error
Sprung mass displacement/(m)	0.05961	0.05759	−3.39%
Gas pressure/(Pa)	424,387	427,470	0.73%
Gas mass flow rate/$(kg{\cdot}s^{-1})$	0.00109	0.00105	−3.67%

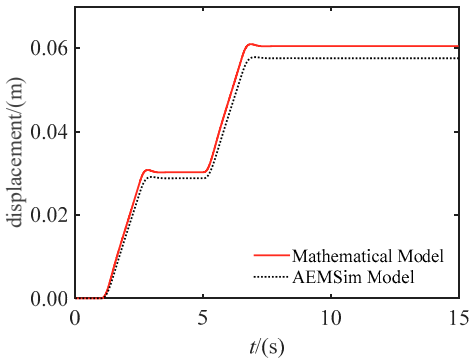

Figure 5. The displacement z_s.

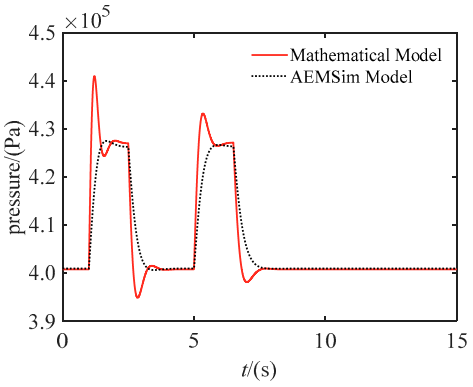

Figure 6. The gas pressure in the airbag.

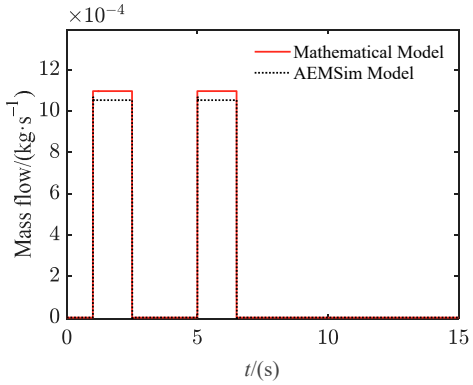

Figure 7. The mass flow.

A comprehensive analysis of Table 3 and Figures 5–7 show that under the same square wave control signal, the responses of both models are consistent. Further comparative analysis shows that although the differences between the steady-state results are small, the differences in the transient process are greater. The main reason for the differences is that there are many simplified conditions in the mathematical model. The comparison results show the validity of the proposed AMESim simulation model. It also shows that the AMESim simulation model can more deeply portray the detailed characteristics of the transient fluctuation of the gas pressure inside the airbag than the mathematical model. Therefore, establishing the AMESim model for trucks will be more helpful in analyzing the process characteristics and detailed features of the vehicle height control strategy. It will help to develop a more practical vehicle height control strategy. Therefore, the following section adopted the ECAS model based on the AMESim software.

3. Modeling of the Half-Truck with the ECAS

3.1. The Dynamic Model of the Half-Truck

The lateral load distribution of the truck in actual operation is more uniform, which has less influence on the frame height adjustment [22]. Therefore, this study carries out research based on the half-truck model, as shown in Figure 8, where m is the sprung mass; z is the vertical displacement at the center of mass; θ is the pitch angle; I_c is the frame moment of inertia; a, b_1, and b_2 are the horizontal distances from the front, middle, and rear axes to the center of mass, respectively; F_{k1} is the spring force of the front suspension; F_{a2} and F_{a3} are the forces of the air springs of the middle suspension and the rear suspension, respectively; and F_{ci} represents the damping force at the corresponding positions, where $i = 1$~3.

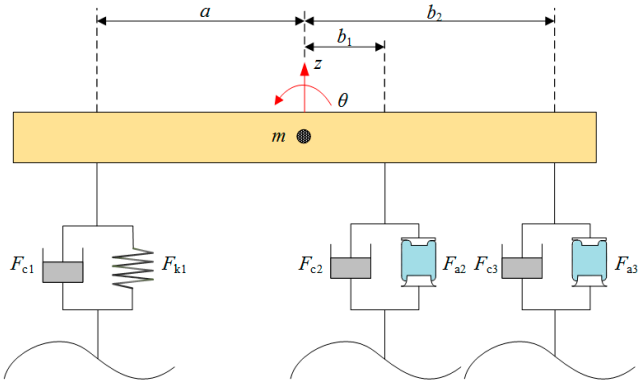

Figure 8. The physical model of the half-vehicle.

Using Newton's second law, the dynamic equations can be expressed as:
(1) The equation of vertical motion:

$$m\ddot{z} = (-F_{c1} - F_{k1} - F_{c2} + F_{a2} - F_{c3} + F_{a3} - mg) \tag{4}$$

(2) The equation of pitch motion:

$$I_c\ddot{\theta} = a(F_{k1} + F_{c1}) + b_1(F_{a2} - F_{c2}) + b_2(F_{a3} - F_{c3}) \tag{5}$$

The frame vertical displacements are at the installation position of each suspension, given that the pitch angle of the truck being studied is small. Formula (6) is allowed to directly use the angle value instead of the sine value of the angle:

$$\begin{cases} x_1 = z - a\theta \\ x_2 = z + b_1\theta \\ x_3 = z + b_2\theta \end{cases} \tag{6}$$

3.2. The Co-Simulation Model of the Half-Truck with the ECAS

The ECAS model for the half-truck is established based on the AMESim software, as shown in Figure 9, respectively. According to the established dynamic equations for the ECAS model based on the AMESim software, the co-simulation model of the half-truck with the ECAS is established based on the Simulink software and the AMESim software, as shown in Figure 10. The information exchange of the force state, the motion state, and control signals is through the Co-simulation Interface module. The parameter settings of the co-simulation model are shown in Table 4 [23], where K_1 is the stiffness of the front suspension, and C_i is the damping coefficient of the corresponding suspension.

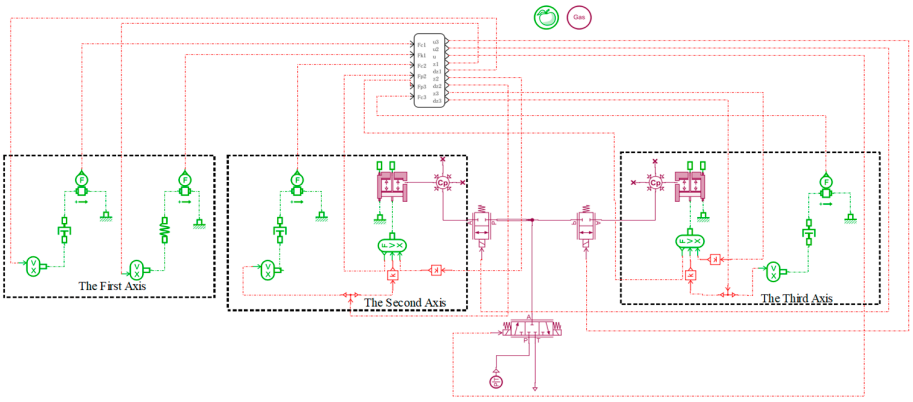

Figure 9. The ECAS model for the half-truck.

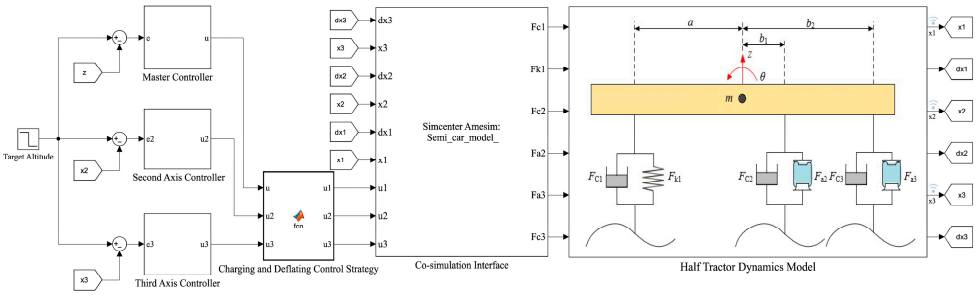

Figure 10. The co-simulation model.

Table 4. Parameter value of the co-simulation model.

Parameter	Value	Parameter	Value
m/kg	6435	b_1/m	0.7620
K_1/(N·m^{-1})	121,306	b_2/m	2.1336
C_1/(N·s·m^{-1})	17,049	I_c/(kg·m^2)	35,711
C_2/(N·s·m^{-1})	28,845	A_e/m^2	4.83×10^{-2}
C_3/(N·s·m^{-1})	28,845	V_{10}/m^3	1.23×10^{-2}
a/m	4.1402	A/m^2	6.23×10^{-6}

4. The Design of the Fuzzy Controller and the Height Control Strategy

4.1. The Design of Fuzzy Controller for the Truck Height

The fuzzy control algorithm, as an empirical and linguistic-based control method, features its core strengths in its formidable adaptability and robustness towards complex systems [24,25]. For systems challenging to articulate precisely with standard mathematical models, such as nonlinear, time-variant systems, and those incorporating uncertain elements, fuzzy control offers an effective control strategy [26–28]. This algorithm can not only manage the uncertainty and complexity inherent in these systems, but also due to its rule-based control logic, it becomes more intuitive and easier for engineers to comprehend and implement [29]. Within the domains of automation and control, especially in electrical control development, the attributes of the fuzzy control algorithm are highly regarded. Facing control systems with intricate structures and where establishing precise mathematical models proves difficult, like the truck electronic control air suspension system, the importance of fuzzy control algorithms becomes particularly pronounced. The truck electronic control air suspension system is structurally complex. It involves intense nonlinearity and time-variant characteristics throughout its operation, making it challenging to achieve the desired control outcomes with traditional control methods. Therefore, this study adopts the fuzzy control algorithm to achieve the frame height control of the truck with the ECAS system.

This study focuses on the frame height regulation. Therefore, the control deviation e and the deviation change rate ec of the body height are defined as the input variables of the fuzzy controller. The output value of the fuzzy controller is the solenoid valve opening u. The fuzzy domain of the input and output variables is set to $[-6, 6]$, as shown in Figure 11. The language describing the input and output fuzzy variables is divided into seven classes: NB (negative large), NM (negative medium), NS (negative small), ZE (zero), PS (positive small), PM (positive medium), and PB (positive large). The triangular affiliation function is selected as the affiliation function for the fuzzy inputs E, EC, and output U, respectively. The fuzzy controller is the Mamdani model, and the center of gravity method is used for clarity to obtain u. The fuzzy control rules are shown in Table 5, and the fuzzy rule surface diagram is shown in Figure 12. The aforementioned design method, once input into MATLAB/Simulink's (2022b) fuzzy logic controller module, can accomplish the software design for the fuzzy controller.

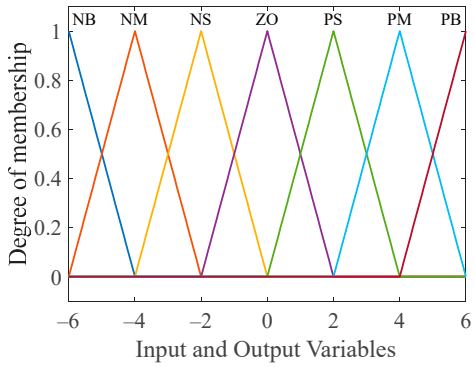

Figure 11. The curves of the affiliation functions.

Table 5. Fuzzy control rules.

EC	*E*						
	NB	**NM**	**NS**	**ZO**	**PS**	**PM**	**PB**
NB	NB	NB	NB	NB	NB	NB	NB
NM	NB	NB	NB	NM	NM	NM	NM
NS	NB	NB	NM	NS	NS	NS	NS
ZO	NM	NM	NS	ZO	PS	PM	PM
PS	PS	PS	PS	PS	PM	PB	PB
PM	PM	PM	PM	PM	PB	PB	PB
PB	PB	PB	PB	PB	PB	PB	PB

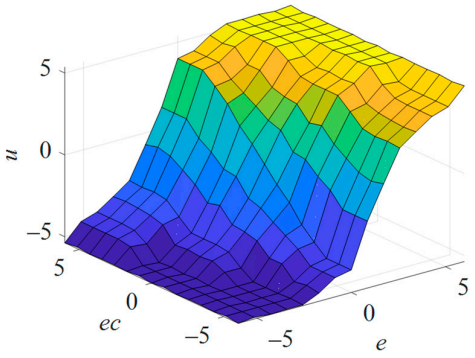

Figure 12. The surface diagram of the fuzzy regular.

4.2. Height Control Strategy of the Truck with the ECAS

4.2.1. The Mode Analysis of the Height Control

The precise control of the frame height of the truck in the parked state can facilitate the loading and unloading of goods, driver boarding, and improving vehicle passability [30]. Considering the actual engineering requirements, the following three typical height control modes are proposed: (1) loading and unloading mode to facilitate the loading and unloading of goods; (2) bad road mode with poor road conditions; (3) high-speed mode to reduce the wind resistance of the body. The target heights of the chassis frame corresponding to the proposed three modes are shown in Table 6.

Table 6. Mode and target height of the frame.

Mode	Frame Height Value	Purpose
Loading and unloading mode	−20.0 mm	Ease of truck handling
Bad path mode	+20.0 mm	Improving truck passability
High-speed mode	−15.0 mm	Improving fuel economy

4.2.2. Design of the Height Control Strategy

Based on the above three height control modes and their corresponding target heights, the following control strategy is proposed to address the frame height adjustment: firstly, the driver selects the appropriate height mode according to the demand; secondly, the actual height of the frame at this time is transmitted to the controller through the sensors, and the controller compares it with the target height under the mode. Finally, the controller transmits the solenoid valve opening signal to the three-position solenoid valve with three-way and the switching valves of the middle and rear axles to complete the frame height adjustment. However, there is the problem of conflicting control sequences of the solenoid valves in the height control process, which aggravates the frame attitude destabilization. To address this problem, a height control strategy is proposed, as shown in Figure 13.

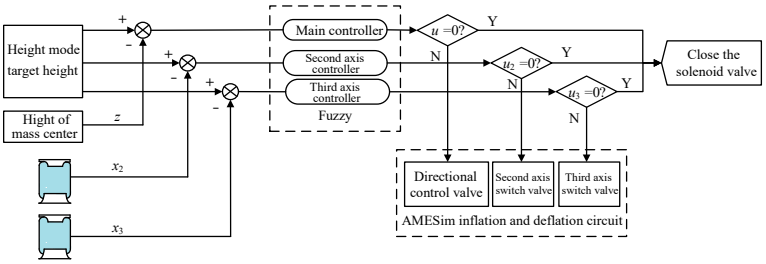

Figure 13. The height control strategy.

As can be seen from Figure 13, when the frame height is lower than the target height, the air springs need to be inflated to raise the vehicle height. However, due to the different loads borne by each air spring, the rising height of the air spring is not consistent. At this time, it can close the switching valve of the air spring below the target height and turn the reversing valve to deflate the air spring above the target height. Until all air springs are below the target height, one must turn the reversing valve again, open the previously closed switching valve, and carry out the inflation operation.

5. Simulation Analysis of the Height Control Strategy for the Truck with the ECAS

According to the frame height control strategy shown in Figure 13, the fuzzy controller is connected to the established co-simulation model of the half-truck. Three typical height adjustment modes were simulated and analyzed on the AMESim/Simulink co-simulation platform; the simulation time was set to 15.0 s, the fixed step size was 0.01 s, and the solver was selected as ode4.

5.1. Height Tracking Performance Analysis

The static equilibrium position of the suspension system is taken as the initial height, and the step target height signal is given at 1.0 s. The simulation results of the loading and unloading mode and the bad road mode are given in the following, as shown in Figures 14 and 15, and Table 7.

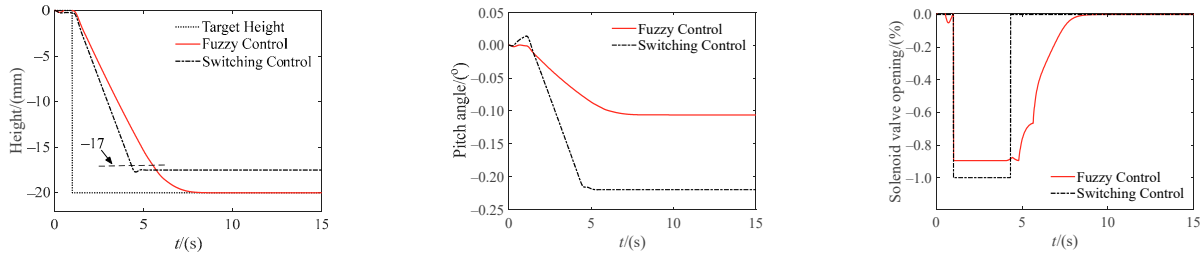

(**a**) (**b**) (**c**)

Figure 14. The loading and unloading mode: (**a**) Frame height; (**b**) Pitch angle; (**c**) Solenoid valve opening.

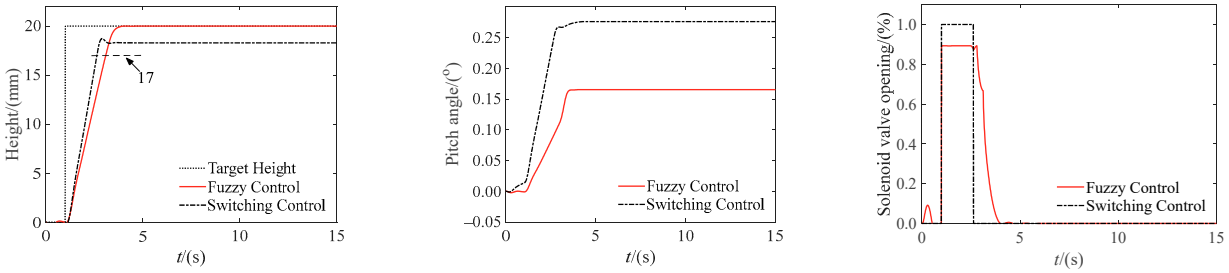

(**a**) (**b**) (**c**)

Figure 15. The bad road mode: (**a**) Frame height; (**b**) Pitch angle; (**c**) Solenoid valve opening.

Table 7. Analysis of co-simulation results.

Performance Analysis		Loading and Unloading Mode		Bad Road Mode	
		Switching	Fuzzy	Switching	Fuzzy
Frame height (mm)	Target height	−20.0		20.0	
	Actual height	−17.5	−19.9	18.3	20.1
	Steady-state error	2.5	0.1	−1.7	0.1
Frame pitch angle (°)	Steady-state value	−0.2	−0.1	0.3	0.2

In the height control mode simulation, the switching controller is used to compare with the fuzzy controller designed in this study. The control logic of the switch control method is as follows: if the current height of the truck's frame deviates from the target frame height by an error greater than the predetermined threshold, the controller issues a control signal. Upon receiving this control signal, the solenoid valve executes either a fully open or fully closed action, thereby inflating or deflating the air springs to adjust the height of the truck's frame accordingly, in which the height dead zone of the switching controller is set to ±3 mm [7]. As shown in Table 7, the height steady-state error and the frame pitch angle steady-state values of the switch controller are less than 2.5 mm and 0.3°, respectively. The height steady-state error and the frame pitch angle steady-state values of the fuzzy controller are less than 0.1 mm and 0.2°, respectively. Compared with the classical switch control method, the control method proposed in this paper can effectively improve the frame height control accuracy by about 10% and reduce the attitude angle by more than 30%.

For the switching controller, after reaching the height dead zone, the solenoid valve is closure. However, due to the inertia of the frame mass and the partial gas pressure for

balancing to overcome the damping force of the damper, it will lead to a brief rise or fall of the frame height, but it is still a large difference with the target height. Figures 14 and 15 clearly depict this phenomenon. The fuzzy controller designed in this study can make real-time fine-tuning of the solenoid valve opening in the process of the frame height lifting and lowering in order to achieve precise control. The frame height response curve can quickly and smoothly converge to the target height without overshooting for the fuzzy controller.

The results show that the fuzzy controller designed, compared with the switch controller, can effectively reduce the steady state error of the frame height control and improve the frame height adjustment accuracy. Moreover, using the proposed control strategy of the frame height adjustment for trucks, the steady state value of the frame pitch angle is smaller, and the frame attitude destabilization caused by the conflict of solenoid valves in the process of air springs inflation and deflation can be effectively avoided.

5.2. Robustness Analysis

To verify the adaptive robustness of the control method proposed in this paper when the truck load changes, we took the sprung mass shown in Table 4 as a benchmark to increase and decrease 30%, respectively. Then, the tracking effect of the target height, which corresponds to the high-speed mode, was compared and analyzed under three different loads conditions. The results are shown in Figure 16. From Figure 16a, it can be seen that the switching control is difficult to effectively suppress the nonlinear characteristics of the air spring inflation and deflation process under different loads, and the target height offset tends to increase with the increase of load. In contrast, it can be seen from Figure 16b that the frame height response curves of the proposed control method in this paper can reach the target height quickly and smoothly, and its steady state error tends to be close to 0, which is almost unaffected by the load change. The results show that the designed fuzzy controller has strong adaptive robustness.

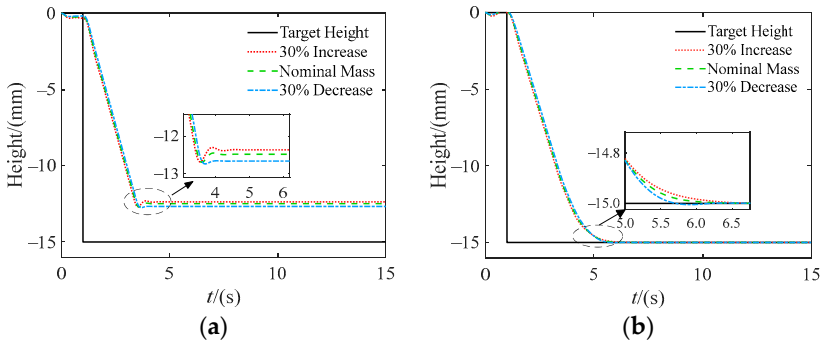

Figure 16. Simulation results of high-speed mode: (**a**) Switching control; (**b**) Fuzzy control.

6. Conclusions

To address the phenomena of large height error and attitude destabilization that occur in the process of regulating the height of trucks with the ECAS, theoretical modeling, control strategy design, simulation verification, and analytical research were carried out, and the main conclusions are as follows:

(1) By comparing the AMESim model and the mathematical model of the single DOF vehicle with the ECAS, it can be concluded that there are significant differences in the transient process of the dynamic response of air springs between the two models. The main reason for the differences is that the mathematical model has more assumptions and simplified conditions. The AMESim model can more deeply portray the detailed characteristics of the transient fluctuation of the gas pressure inside the air spring than the mathematical model. (2) The co-simulation model of the half-truck with the ECAS was constructed, which provides a more refined dynamic model for the design and effectiveness verification of the height control strategies for trucks with the ECAS. (3) Based on the fuzzy control theory, a fuzzy controller of the frame height is designed, and three typical height

control modes and control strategies are proposed based on the requirements of the truck's actual use scenarios. These form a relatively complete height control method for trucks with the ECAS. (4) The simulation analysis results show that the proposed control method has better control effectiveness and robustness. It can effectively reduce the height error and avoid the attitude destabilization in the control process of the ECAS.

Author Contributions: Data curation, H.Z. (Hao Zhang 1); Formal analysis, H.Z. (Hao Zhang 1); Funding acquisition, L.Z. and C.O.; Investigation, L.Z.; Methodology, C.O.; Software, Y.L.; Writing—original draft, H.Z. (Hao Zhang 2); Writing—review and editing, X.S. All authors have read and agreed to the published version of the manuscript.

Funding: This work was supported by the Opening Project of Key Laboratory of operation safety technology on transport vehicles, Ministry of Transport, PRC (KFKT2022-04), the Shandong Province High Quality Professional Degree Teaching Case Library Construction Project (SDYAL2023113).

Data Availability Statement: The original contributions presented in the study are included in the article, further inquiries can be directed to the corresponding author.

Conflicts of Interest: The authors declare no conflicts of interest.

References

1. Fu, S.; Xu, Y.H.; Sun, Z.B. Overview of the development of automobile air suspension system and precise control technology. *Chin. Hydraul. Pneum.* **2023**, *47*, 107–114.
2. Liu, D.X. Research on partial revision related to bus for technical specifications for safety of power-driven vehicles operating on roads. *Automob. Appl. Technol.* **2018**, *6*, 162–163.
3. Xu, X.; Chen, L.; Jiang, X.W.; Liang, C.; Wang, F. Semi-active control of Quasi-zero stiffness air suspension system for commercial vehicles based on H_∞ state feedback. *J. Mech. Eng.* **2023**, *59*, 306–317.
4. Zhu, H.J.; Yang, J.; Zhang, Y.Q. Dual-chamber pneumatically interconnected suspension: Modeling and theoretical analysis. *Mech. Syst. Signal Process.* **2021**, *147*, 107125. [CrossRef]
5. Yang, C.; Peterson, A.W.; Ahmadian, M. Achieving anti-roll bar effect through air management in commercial vehicle pneumatic suspensions. *Veh. Syst. Dyn.* **2019**, *57*, 1775–1794.
6. Sun, X.Q.; Yuan, C.C.; Cai, Y.F.; Wang, S.H.; Chen, L. Model predictive control of an air suspension system with damping multi-mode switching damper based on hybrid model. *Mech. Syst. Signal Process.* **2017**, *94*, 94–110. [CrossRef]
7. Yin, H.; Wu, M.Y.; Li, X.B.; Lu, J.C.; Du, Y.C.; Liang, G.Q.; Wei, Y.T. Sliding mode control of air suspension height with Dual-Deadband design. *Eng. Mech.* **2022**, *39*, 209–218.
8. Zhu, H.J.; James, Y.; Zhang, Y.Q.; Feng, X.X. A novel air spring dynamic model with pneumatic thermodynamics, effective friction and viscoelastic damping. *J. Sound Vib.* **2017**, *408*, 87–104. [CrossRef]
9. Xu, L.F. Mathematical modeling and characteristic analysis of the vertical stiffness for railway vehicle air spring system. *Math. Probl. Eng.* **2020**, *2020*, 2036563. [CrossRef]
10. Sayyaadi, H.; Shokouhi, N. Effects of air reservoir volume and connecting pipes' length and diameter on the air spring behavior in Rail–Vehicles. *Iran. J. Sci. Technol. B* **2010**, *34*, 499–508.
11. Chen, Y.; Zhang, S.; Mao, E.R.; Du, Y.F.; Chen, J.; Yang, S.J. Height stability control of a large sprayer body based on air suspension using the sliding mode approach. *Inf. Process. Agric.* **2020**, *7*, 20–29. [CrossRef]
12. Kim, H.; Lee, H. Height and leveling control of automotive air suspension system using sliding mode approach. *IEEE Trans. Veh. Technol.* **2011**, *60*, 2027–2041.
13. Ma, X.B.; Wong, P.K.; Zhao, J.; Zhong, J.H.; Ying, H.; Xu, X. Design and testing of a nonlinear model predictive controller for ride height control of automotive Semi-Active air suspension systems. *IEEE Access* **2018**, *6*, 63777–63793. [CrossRef]
14. Kou, F.R.; He, L.L.; Tian, L.; Chen, C.; Hong, F. Multi-mode Coordination Control of the Hybrid Air Suspension. *Chin. Hydraul. Pneum.* **2020**, *4*, 15–22.
15. Li, Z.X.; Wu, M.Y.; Zhou, F.Q.; Wei, Y.T. Modeling of air spring and its height control strategy. *J. Mech. Electr. Eng.* **2022**, *39*, 53–58.
16. Akpakpavi, M.; Jiang, H. Modeling, Simulation and Body Height Adjustment Control of Full Car Laterally Interconnected Air Suspension System. *Int. Ref. J. Eng. Sci.* **2017**, *6*, 31–42.
17. Hu, Q.; Lu, W.; Jiang, J. Design of a Vehicle Height and Body Posture Adjustment Hybrid Automaton of Electronically Controlled Air Suspension. *Adapt. Control Signal* **2021**, *35*, 1879–1897. [CrossRef]
18. Zhao, R.C.; Xie, W.; Yu, G.; Wang, G.W.; Wong, P.A.; Silvestre, C. Adaptive ride height controller design for vehicle active suspension systems with uncertain sprung mass and Time-varying disturbances. *Int. J. Robust Nonlinear Control* **2022**, *32*, 5950–5966. [CrossRef]
19. Sun, L.Q.; Wang, Y.; Li, Z.X.; Geng, G.Q.; Liao, Y.G. H_∞ Robust control of interconnected air suspension based on mode switching. *IEEE Access* **2022**, *10*, 62377–62390. [CrossRef]
20. Shalabi, M.E.; Fath Elbab, A.M.R.; El-Hussieny, H.; Abouelsoud, A.A. Neuro-Fuzzy volume control for quarter car Air-Spring suspension system. *IEEE Access* **2021**, *9*, 77611–77623. [CrossRef]

21. Xiao, F.; Chen, L.; Wang, S.H.; Sun, X.Q. Research on fuzzy self adaptive control of ECAS vehicle height adjustment system based on AMESim. *Mach. Des. Manuf.* **2016**, *302*, 141–144.
22. Zhao, L.L.; Yu, Y.W.; Zhou, C.C.; Huang, D.H.; Yuan, J. Pitching-Plane dynamics model of heavy truck cab considering constraints of guiding swing arm. *Automot. Eng.* **2021**, *43*, 136–144.
23. Chen, Y.; Ahmadian, M.; Peterson, A. Pneumatically Balanced Heavy Truck Air Suspensions for Improved Roll Stability. In *SAE 2015 Commercial Vehicle Engineering Congress*; SAE: Detroit, MI, USA, 2015; p. 11.
24. Nguyen, T.A. Preventing the Rollover Phenomenon of the Vehicle by Using the Hydraulic Stabilizer Bar Controlled by a Two-Input Fuzzy Controller. *IEEE Access* **2021**, *9*, 129168–129177. [CrossRef]
25. Jia, T.; Pan, Y.; Liang, H.; Lam, H.K. Event-Based Adaptive Fixed-Time Fuzzy Control for Active Vehicle Suspension Systems With Time-Varying Displacement Constraint. *IEEE Trans. Fuzzy Syst.* **2022**, *30*, 2813–2821. [CrossRef]
26. Mahmoodabadi, M.J.; Nejadkourki, N. Optimal Fuzzy Adaptive Robust PID Control for an Active Suspension System. *Aust. J. Mech. Eng.* **2022**, *20*, 681–691. [CrossRef]
27. Golouje, Y.N.; Abtahi, S.M. Chaotic Dynamics of the Vertical Model in Vehicles and Chaos Control of Active Suspension System via the Fuzzy Fast Terminal Sliding Mode Control. *J. Mech. Sci. Technol.* **2021**, *35*, 31–43. [CrossRef]
28. Swethamarai, P.; Lakshmi, P. Adaptive-Fuzzy Fractional Order PID Controller-Based Active Suspension for Vibration Control. *IETE J. Res.* **2022**, *68*, 3487–3502. [CrossRef]
29. Gao, Z.P.; Nan, J.R.; Liu, L.; Xu, X.L. Research on air suspension control system based on fuzzy control. *Energy Procedia* **2017**, *105*, 2653–2659.
30. Zheng, Y.Q.; Shangguan, W.B.; Rakheja, S. Modeling and performance analysis of convoluted air springs as a function of the number of bellows. *Mech. Syst. Signal Process.* **2021**, *159*, 107858. [CrossRef]